SciPost Phys. Proc. 17, 022 (2025)

Measurement of the muon magnetic anomaly to 0.20 ppm by the Muon g-2 experiment at Fermilab

Lorenzo Cotrozzi, on behalf of the Muon g-2 collaboration

Department of Physics, University of Liverpool, UK
INFN, Pisa, Italy

lcotrozz@hep.ph.liv.ac.uk

The 17th International Workshop on Tau Lepton Physics (TAU2023)
Louisville, USA, 4-8 December 2023
doi:10.21468/SciPostPhysProc.17

Abstract

The Muon $g-2$ experiment at Fermilab aims to measure the muon magnetic moment anomaly, $a_\mu = (g-2)/2$, with a final accuracy of 0.14 parts per million (ppm). The experiment's first result was published in 2021, based on data collected in 2018, and in 2023 a new result was published based on two more years of data taking, 2019 and 2020. The combination of the two results from Fermilab and the previous one from Brookhaven National Laboratory brought the uncertainty on the experimental measurement of a_μ to the unprecedented value of 0.19 ppm. This paper will present details about the improvements of statistical and systematic uncertainties on a_μ since the 2021 result.

Received 2024-07-04
Accepted 2024-12-27
Published 2025-07-23
doi:10.21468/SciPostPhysProc.17.022

1 The magnetic moment of the muon

The gyromagnetic ratio g is a factor of proportionality between the magnetic moment $\vec{\mu}$ of a charged particle and its spin $\vec{S}$: $\vec{\mu} = g(e/2m)\vec{S}$. From Dirac's equation, muons should have a value of g equal to 2; but in the Standard Model (SM) framework of quantum field theories, g is corrected to a slightly higher value than 2 from QED, weak interactions and QCD. The muon magnetic anomaly is defined as the fractional difference of g_μ from 2: $a_\mu = (g_\mu - 2)/2$. Figure 1 presents the experimental values of a_μ as measured by BNL E821 [1] and FNAL E989 in Run-1 (2021) [2] and Run-2/3 (2023) [3, 4]. The contribution to a_μ from the quantum chromodynamics (QCD) sector amounts to ~ 60 parts per million (ppm) and carries the largest uncertainty. The major contribution comes from hadronic vacuum polarization (HVP), where the energy scale is of the order of the muon mass, well below the region where QCD can be studied perturbatively: a dispersion relation approach can be used to evaluate the contribution, using the experimental hadronic cross section of e^+e^- as an input. Lattice QCD can also be used to determine the HVP contribution to a_μ using an ab-initio calculation. In 2020, the

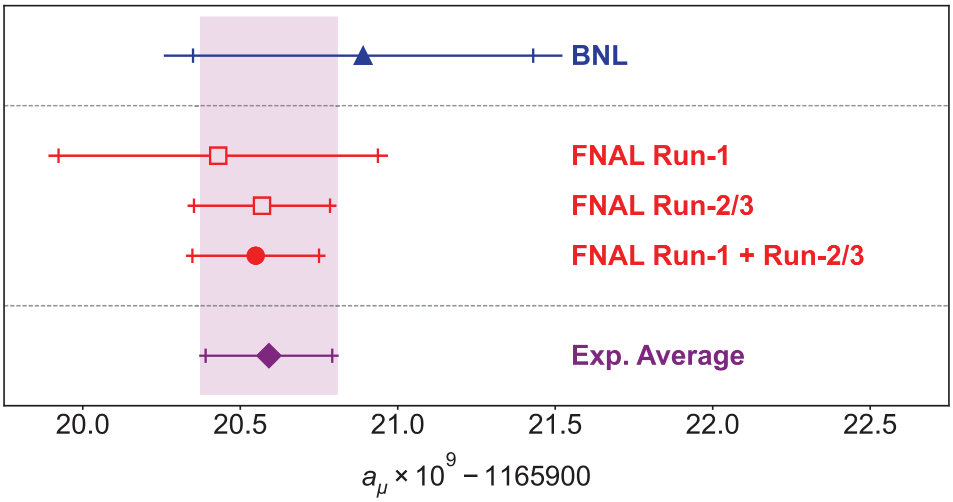

Figure 1: Measured values of a_μ from BNL and FNAL, and new experimental average. The inner tick marks indicate the statistical contribution to the total uncertainties [3].

Theory Initiative recommended a value for the theoretical prediction of a_μ in a White Paper [5], based on the dispersive approach. This led to a discrepancy between the experimental value and the SM calculation from the Muon $g-2$ Theory Initiative: $a_\mu^{exp} - a_\mu^{SM} = (249 \pm 48) \cdot 10^{-11}$, with a significance of $5.1\,\sigma$. In recent years, puzzles in the theoretical prediction of a_μ have arisen, which prevent a solid comparison with the experimental value. In 2021, the BMW collaboration presented a prediction of a_μ^{HVP} with lattice QCD with an uncertainty of 0.8% [6], which was in tension with the dispersive approach. Other collaborations which use a lattice approach are working to reach a similar uncertainty on a_μ^{HVP} as BMW, in order to verify the current prediction. On top of that, in 2023 the measurement of the $e^+e^- \to \pi^+\pi^-$ cross section with the CMD-3 detector [7] resulted in a hadronic contribution to a_μ that was significantly larger than the value obtained from previous measurements.

2 The Muon $g-2$ (E989) experiment at Fermilab

In the Muon $g-2$ experiment, a spin-polarized beam of 3.1 GeV positively charged muons is injected into a $\sim$ 7 m radius superconducting storage ring, that produces a vertical and uniform, at the ppm level, 1.45 T magnetic field. Electrostatic quadrupole (ESQ) plates provide weak focusing for vertical confinement. In the storage ring, muons precess with cyclotron frequency ω_C, and their spin also precesses around the direction of the magnetic field, with frequency ω_S. Given e and m the charge and mass of muons, respectively, the anomalous precession frequency ω_a is defined as:

$$\vec{\omega}_a \equiv \vec{\omega}_S - \vec{\omega}_C = -\frac{e}{m}\left[a_\mu \vec{B} - a_\mu \left(\frac{\gamma}{\gamma+1}\right)(\vec{\beta}\cdot\vec{B})\vec{\beta} - \left(a_\mu - \frac{1}{\gamma^2-1}\right)\frac{\vec{\beta}\times\vec{E}}{c}\right]. \tag{1}$$

$\vec{E}$ is the electric field from ESQ, $\vec{B}$ the magnetic dipole, $\vec{\beta}$ the muons' speed and γ their Lorentz factor. In the Muon $g-2$ experiment, only the first term in square brackets is relevant in the first approximation, because muons travel perpendicularly to the B-field and $\gamma \approx 29.3$ is such that the last parenthesis vanishes. When only the first term is considered, the equation for $\vec{\omega}_a$ becomes $\omega_a = a_\mu (e/m) B \simeq 1.43\,\mathrm{rad}/\mu\mathrm{s}$, with a direct proportionality between a_μ and ω_a/B. Expressing the magnetic field in terms of the Larmor precession frequency of free protons, via

$\hbar\omega_p = 2\mu_p|\vec{B}|$, the formula used for a_μ is in Equation (2):

$$a_\mu = \left[\frac{f_{\text{clock}} \cdot \omega_a \left(1 + C_e + C_p + C_{pa} + C_{dd} + C_{ml}\right)}{f_{\text{calib}} \cdot \langle \omega'_p(\vec{r}) \times M(\vec{r}) \rangle \left(1 + B_q + B_k\right)} \right] \times \frac{\mu_p(T_r)}{\mu_e(H)} \frac{\mu_e(H)}{\mu_e} \frac{m_\mu}{m_e} \frac{g_e}{2} \,. \tag{2}$$

Inside the square brackets, at the numerator, ω_a is the anomalous precession frequency, measured as described in Subsection 2.1; the factor f_{clock}, unknown to the Muon g−2 collaboration, is set to introduce a blinding in the range ± 25 ppm; the measurement of the magnetic field factor at the denominator $f_{\text{calib}} \cdot \langle \omega'_p(\vec{r}) \times M(\vec{r}) \rangle$ is described in Subsection 2.2, where the prime symbol $'$ indicates shielded (not free) protons; the factors C_i and B_i account for beam dynamics and magnetic transients effects, respectively, and are described in Subsection 2.3. The external factors are known to 25 parts per billion (ppb) [4], and they are: the shielded proton-to-electron magnetic moment $\mu_p(T_r)/\mu_e(H)$, measured at the refence temperature of $T_r = 34.7\,°\text{C}$; the QED factor $\mu_e(H)/\mu_e$, which is the ratio of the magnetic momentum of the electron in a hydrogen atom to the magnetic momentum of the free electron in vacuum; the ratio between the muon and electron masses m_μ/m_e, and the electron g-factor g_e.

2.1 ω_a measurement

24 electromagnetic calorimeters are placed along the inner radius of the Muon $g-2$ storage ring, each composed of an array of 6×9 lead-fluoride crystals, that can detect positrons from μ^+ decays. Positrons generate Cherenkov light in the crystals, which is detected by SiPMs, converted into a voltage signal and recorded for analysis. From template fits on crystal pulses, positrons' energies and times of arrival are reconstructed. Since muons decay weakly, there is a correlation between the positron energy in the center-of-mass frame and the direction of the muon spin. In the lab frame, the time distribution of positrons above a given threshold is given by Equation (3):

$$N(t) = N_0 e^{-t/\gamma\tau} \left[1 + A_0 \cos(\omega_a t + \phi_0)\right] , \tag{3}$$

where N_0 is a normalization parameter, A_0 the amplitude of the oscillation, ϕ_0 the initial phase, and $\gamma\tau$ is the muon lifetime in the lab frame. We choose a threshold of 1.7 GeV that minimizes the statistical uncertainty on ω_a. In alternative, it is possible to weight the contribution of each event by the asimmetry A, which depends on the positron energy E, which enable us to lower the threshold down to 1 GeV thus increasing the statistics and reducing the uncertainty. The complete ω_a fit function includes terms which account for the muon losses and beam dynamics frequencies; the number of floating parameters depends on the analysis group, and is typically between 20 and 30 [4].

2.2 Magnetic field measurement

During data taking, the proton precession ω'_p is constantly measured by 378 nuclear magnetic resonance (NMR) fixed probes, placed along the ring above and below the storage volume. About once every three days, a so-called *trolley run* is performed with no muon beam stored, where a cylinder equipped with 17 NMR probes is moved on rails inside the vacuum chamber with the purpose of producing a three dimensional map of the magnetic field that the muons experience. The fixed probes monitor the field stability between two consecutive trolley runs. The NMR technique uses a radio frequency (RF) pulse ($\sim$ 61 MHz) applied to the proton sample in petroleum jelly, in order to rotate the proton spin of 90° such that it lies in the plane perpendicular to the storage ring B-field. When the RF pulse is turned off, the sample polarization starts precessing in the storage ring magnetic field until the net magnetization of the sample returns to being aligned with the external field. Pickup coils oriented perpendicularly to the magnetic field are connected to waveform digitizers that save the current induced in the coils by the precessing protons: this current is the so-called free induction decay signal, and measuring it over time gives information about the magnetic field. The Larmor precession frequency is about 61.79 MHz in the $g-2$ storage ring, and it is mixed down to ~ 50 kHz prior to digitization. Both the trolley and fixed probes are calibrated with a water-sample probe, that can be positioned in the same locations as the trolley probes. This step provides the absolute calibration of the field measurement represented by the term f_{calib} in Equation (2). The term f_{calib} includes the effects related to the diamagnetic shielding of the petroleum jelly NMR probes caused by the trolley body and shape. The final value of ω'_p required in Equation (2) is the average magnetic field $\tilde{\omega}'_p$ experienced by the muons as they precess around the ring, obtained by weighting the ω'_p map with the muon beam distribution $M(\vec{r}, t)$ measured by two straw tracker detectors, and by integrating over time and space [4].

2.3 Beam dynamics and transient fields corrections

The anomalous precession frequency ω_a is extracted from wiggle plot fits. The quantity that we measure, indicated with ω_a^m in Equation (2), is not truly the precession frequency ω_a due to beam dynamics effects which modify the simple relation $\omega_a = a_\mu(e/m)B$. The electric field C_e and pitch C_p corrections make the spin precess slower than in the ideal experiment; the phase acceptance C_{pa}, differential decay C_{dd} and muon losses C_{ml} corrections affect the average muon initial phase ϕ of Equation (3) over fill time, thus biasing ω_a. The corrections B_k and B_q arise because, during muon storage, two time-dependent magnetic fields are induced by the pulsed magnetic and electric fields from the kicker and quadrupoles that are synchronized with each muon fill. These transient magnetic fields are not present during the trolley runs; the fixed probes only measure the field at time intervals of ~ 1 s asynchronously with respect to muon injection, whereas the fast transients change on the µs timescales, so they must be included as corrections to ω_p at the denominator of Equation (2). In paragraphs V and VI.G of the PRD article [4], these corrections are described in detail: their overall contribution is 0.6 ppm, which is ~ 5 times larger than the uncertainty we plan to quote with the full statistics.

3 Improvements from Run-1 to Run-2/3 results

There were several improvements after the Run-1 (2021) result, in terms of running conditions, analysis techniques and systematic studies. First of all, in Run-2/3 we collected 4.7 times the number of Run-1 decay positrons, which reduced the statistical uncertainty on ω_a by a factor ~ 2.2, and allowed to perform more detailed studies on one of the systematic effects that dominated the Run-1 results, namely the aliased Coherent Betatron Oscillation of the muon beam. During Run-1 there were two damaged resistors in the ESQ plates, fixed before Run-2, which strongly affected the stability of beam oscillations and enhanced the phase acceptance correction C_{pa} and its uncertainty. Towards the end of Run-3, the non-ferric fast kicker magnet, which is necessary to store the muon beam at the time of injection, was upgraded in order to achieve the optimal kick, consequently lowering the electric field correction C_e. On the ω_a side, new reconstruction algorithms were employed to reduce the pileup systematic uncertainty, which dominated in Run-1. In addition, a new Asymmetry-weighted ratio method was developed, which consisted in subdividing data into two wiggle plots, weighting the positron events and shifting them in time appropriately such that the ratio between their difference and their sum cancelled the muon exponential decay. This method preserved statistical power in the ω_a fit, whilst reducing sensitivity to many systematics. On the field side, more measure-

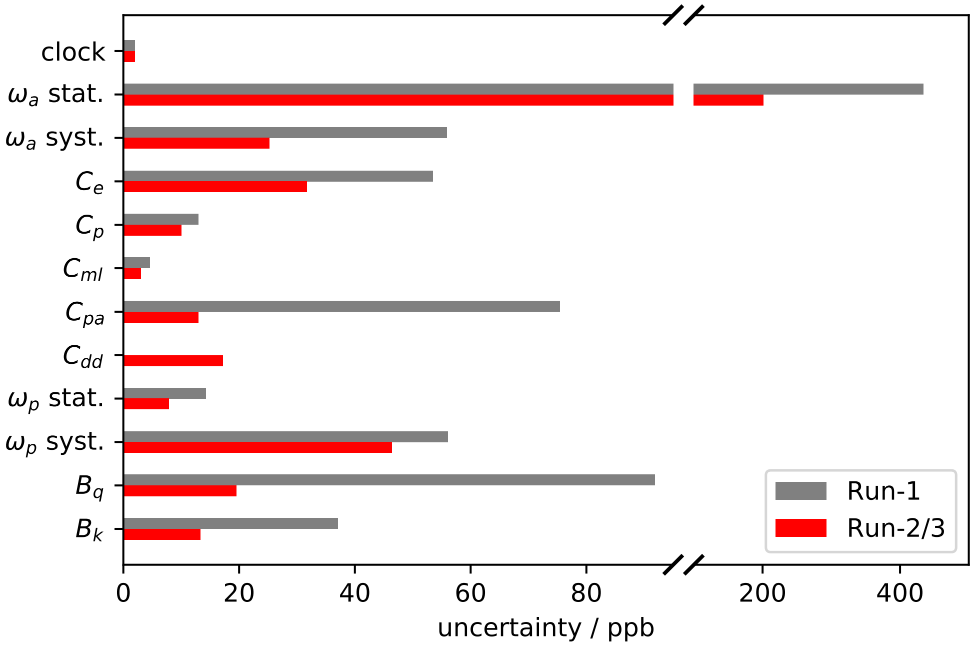

Figure 2: Comparison of statistical and systematic uncertainties between the Run-1 [2] and the Run-2/3 [3,4] results.

ments of the quadrupole transients and improvements in the magnetometer that measured the kicker transients resulted in smaller systematic uncertainties for the respective terms B_q and B_k. With all these improvements, in Run-2 and Run-3 the statistical and systematic uncertainties on a_μ were reduced with respect to Run-1, from 434 ppb to 201 ppb and from 157 ppb to 70 ppb, respectively. Figure 2 shows the improvements in individual terms of Equation (2).

4 Conclusion

The goal of the Muon $g-2$ experiment at Fermilab is to measure the muon magnetic anomaly a_μ at the 0.14 ppm level of precision, a fourfold improvement with respect to the previous experiment at BNL. Combining the experiment's results of 2021 and 2023 and the previous BNL result, the new experimental measurement of a_μ has reached the unprecedented precision of 0.19 ppm; in the 2023 result, the systematic uncertainty reached 70 ppb, surpassing the goal of 100 ppb [8], and with the ongoing analysis of the last three datasets, Run-4/5/6, we expect to reach the goal of 100 ppb in statistical uncertainty.

Acknowledgments

Funding information This work was supported in part by the US DOE, Fermilab, the Istituto Nazionale di Fisica Nucleare and the European Union Horizon 2020 research and innovation programme under the Marie Skłodowska-Curie grant agreements No. 101006726, No. 734303.

References

[1] G. W. Bennett et al., *Final report of the E821 muon anomalous magnetic moment measurement at BNL*, Phys. Rev. D **73**, 072003 (2006), doi:10.1103/PhysRevD.73.072003.

[2] B. Abi et al., *Measurement of the positive muon anomalous magnetic moment to 0.46 ppm*, Phys. Rev. Lett. **126**, 141801 (2021), doi:10.1103/PhysRevLett.126.141801.

[3] D. P. Aguillard et al., *Measurement of the positive muon anomalous magnetic moment to 0.20 ppm*, Phys. Rev. Lett. **131**, 161802 (2023), doi:10.1103/PhysRevLett.131.161802.

[4] D. P. Aguillard et al., *Detailed report on the measurement of the positive muon anomalous magnetic moment to 0.20 ppm*, Phys. Rev. D **110**, 032009 (2024), doi:10.1103/PhysRevD.110.032009.

[5] T. Aoyama et al., *The anomalous magnetic moment of the muon in the Standard Model*, Phys. Rep. **887**, 1 (2020), doi:10.1016/j.physrep.2020.07.006.

[6] Sz. Borsanyi et al., *Leading hadronic contribution to the muon magnetic moment from lattice QCD*, Nature **593**, 51 (2021), doi:10.1038/s41586-021-03418-1.

[7] F. V. Ignatov et al., *Measurement of the $e^+e^- \to \pi^+\pi^-$ cross section from threshold to 1.2 GeV with the CMD-3 detector*, Phys. Rev. D **109**, 112002 (2024), doi:10.1103/PhysRevD.109.112002.

[8] J. Grange et al., *Muon $(g-2)$ technical design report*, (arXiv preprint) doi:10.48550/arXiv.1501.06858.